

1  
2  
3  
4  
5  
6  
7  
8  
9  
10  
11  
12  
13  
14  
15  
16  
17  
18  
19  
20  
21  
22  
23  
24  
25  
26  
27  
28  
29  
30  
31  
32  
33  
34

# Eliciting a potent antitumor immune response by expressing tumor antigens in a skin commensal

Y. Erin Chen<sup>1,2,3,5</sup>, Katayoon Atabakhsh<sup>1,2,3</sup>, Alex Dimas<sup>1,2,3</sup>, Kazuki Nagashima<sup>1,2,3</sup>, Michael A. Fischbach<sup>1,2,3,4\*</sup>

<sup>1</sup>Department of Bioengineering, Stanford University, Stanford, CA 94305, USA

<sup>2</sup>Department of Microbiology & Immunology, Stanford University School of Medicine, Stanford, CA 94305, USA

<sup>3</sup>ChEM-H Institute, Stanford University, Stanford, CA 94305, USA

<sup>4</sup>Chan Zuckerberg Biohub, Stanford, CA 94305, USA

<sup>5</sup>Dermatology Service, San Francisco Veterans Administration Health Care System, San Francisco, CA, USA

\*Correspondence: [fischbach@fischbachgroup.org](mailto:fischbach@fischbachgroup.org)

35 **ABSTRACT**

36 Immune modulation has become central to treating cancer. However, global immune  
37 stimulation is only effective in a subset of patients and can lead to serious complications, including  
38 colitis and type I diabetes. Newer modalities like engineered T cells and tumor vaccines are more  
39 specific, but they have shown limited efficacy in solid tumors and are difficult to scale. Bacterial  
40 strains from the human microbiome can induce antigen-specific T cells to help maintain barrier  
41 function. Here, we redirect CD8+ and CD4+ T cells elicited by the skin commensal *Staphylococcus*  
42 *epidermidis* to recognize tumor cells by expressing tumor-derived antigens in the bacterial cell. *S.*  
43 *epidermidis* expressing the model antigen ovalbumin (*S. epidermidis*-OVA) stimulates antigen-  
44 specific CD8+ and CD4+ T cells in vitro. The subcellular localization of the antigen skews the  
45 response: cell wall-attached OVA preferentially stimulates CD8+ T cells whereas secreted OVA  
46 predominantly induces CD4+ T cells. In a syngeneic tumor model (OVA-expressing B16  
47 melanoma), mice colonized topically with *S. epidermidis*-OVA exhibit a marked reduction in  
48 subcutaneous tumor volume compared to mice colonized with *S. epidermidis* expressing mCherry;  
49 this effect is dependent on live bacteria and a combination of CD8+ and CD4+ T cells. *S.*  
50 *epidermidis*-OVA also reduces tumor burden when tumor cells are injected intravenously (a model  
51 of metastasis), demonstrating that the antitumor effect operates in tissues distant from the site of  
52 bacterial colonization. *S. epidermidis* strains expressing neoantigen peptides from the B16 tumor  
53 cell line exhibit potent antitumor efficacy without inducing an autoimmune response against  
54 melanocytes in healthy tissue. Antigen-expressing colonists are a simple but powerful strategy to  
55 elicit a targeted T cell response in the context of cancer and other diseases.

## 56 MAIN TEXT

57 Immune modulation has become a central component of cancer therapies, with inhibitors of the  
58 checkpoint proteins PD-1 and CTLA-4 most widely deployed<sup>1</sup>. Although checkpoint blockade is efficacious  
59 across many cancer types, it only works in a subset of patients. Moreover, global stimulation of immune  
60 function frequently induces autoimmunity (e.g., colitis and type 1 diabetes)<sup>2,3</sup>. Thus, a central challenge in  
61 immuno-oncology is to develop methods for stimulating immune cells that recognize cancer cells  
62 selectively.

63 There are two predominant strategies for eliciting specific immune responses in the context of  
64 oncology. The first is to generate antigen-specific T cells by ex vivo transduction or electroporation with a  
65 chimeric antigen receptor (CAR) or a T cell receptor (TCR)<sup>4,5</sup>. This approach has shown great promise in  
66 treating hematologic malignancies but has several downsides: it is expensive<sup>6</sup>, engineered T cells can be  
67 prone to exhaustion<sup>7</sup>, and there have been challenges in getting CAR-T cells to act against solid tumors<sup>8</sup>.  
68 The second strategy is to vaccinate the host with tumor neoantigens or antigen-loaded dendritic cells;  
69 these approaches have yielded promising results in preclinical models but are not yet consistently  
70 efficacious in clinical trials<sup>9-12</sup>.

71 Certain strains of the gut and skin microbiota induce antigen-specific T cells<sup>13-16</sup>, raising the  
72 possibility of a simpler way to elicit a targeted T cell response that does not require ex vivo cell engineering.  
73 However, the T cells induced by the microbiota harbor TCRs specific for bacterial antigens, limiting their  
74 utility in treating cancer or autoimmune disease. Here, we show that this process can be redirected to elicit  
75 antigen-specific T cells against non-bacterial antigens. By expressing a model antigen or a tumor-derived  
76 neoantigen in the T cell-stimulatory skin commensal *Staphylococcus epidermidis* LM087, we elicit tumor-  
77 specific CD8+ and CD4+ T cells. These cells protect against local and metastatic progression of a poorly  
78 immunogenic mouse melanoma.

79

### 80 **Selecting *Staphylococcus epidermidis* LM087 as the tumor antigen chassis**

81 Previous efforts to engineer a bacterial strain to elicit an antitumor response have involved the  
82 pathogens *Listeria monocytogenes* and *Salmonella typhimurium*. In both cases, antigen-specific T cell  
83 responses leading to tumor regression have been observed<sup>17,18</sup>. However, the antitumor efficacy of  
84 *Listeria*- and *Salmonella*-based vaccines relies on nonspecific immune activation resulting from local tissue  
85 damage, infection and replication within antigen-presenting cells, or direct infection of tumor cells<sup>19</sup>. Efforts  
86 have been made to attenuate each pathogen to alleviate the toxicity of infection, but attenuation typically  
87 dampens the desired immune response<sup>19</sup>. Efforts to use non-pathogenic *Escherichia coli* strains to boost  
88 antitumor immunity also hold promise, but require intratumoral delivery<sup>20,21</sup>.

89 We decided instead to work with a prevalent member of the healthy human skin microbiome.  
90 *Staphylococcus epidermidis* LM087 induces antigen-specific CD8+ T cells in mice and non-human

91 primates<sup>15,22,23</sup>. Importantly, it does so in the context of physiologic skin colonization—without mounting an  
92 infection, breaching the skin barrier, or causing any pathologic response. This strain colonizes the skin for  
93 an extended period of time after a single application; the CD8+ T cell response it elicits in mice is durable  
94 for nine months<sup>22</sup>. We hypothesized that *S. epidermidis* could be a promising starting point for eliciting  
95 antitumor immunity given its lack of toxicity and the specificity and potency of the CD8+ T cell response  
96 observed in mice and non-human primates following topical application.

97

## 98 **Developing a genetic system for *S. epidermidis***

99 Despite the fact that *S. epidermidis* colonizes the skin of every human, methods to manipulate it  
100 genetically are poorly developed; only a handful of mutants have ever been reported, and only in strains  
101 that adsorb phage efficiently or are domesticated<sup>24,25</sup>.

102 Targeted genetic modification of *S. epidermidis* has been challenging for two reasons: *S.*  
103 *epidermidis* has multiple stringent restriction systems that differ substantially among strains<sup>24,26,27</sup>, and—  
104 as with many other Gram-positive bacteria—electroporation is an inefficient means of introducing DNA,  
105 owing to the thick cell wall<sup>28</sup>. To bypass poor electroporation efficiency, a genetic approach was recently  
106 described that involves transduction with bacteriophage  $\Phi$ 187 from an engineered restriction-deficient *S.*  
107 *aureus* (PS187  $\Delta$ *hdsR*  $\Delta$ *sauPSI*) to *S. epidermidis* or other coagulase-negative *Staphylococcus* species  
108 on the basis of their similarity in wall teichoic acid structure<sup>29,30</sup>. Although this method works well for a  
109 specific clade of *S. epidermidis* strains, it is time-consuming, requires prolonged phage propagation, and  
110 is useful only for certain strains of *S. epidermidis* with efficient phage adsorption capacity. Given the high  
111 variability of phage specificity across *S. epidermidis* strains, there are many primary isolates of *S.*  
112 *epidermidis* for which this method does not work.

113 Reasoning that antigen engineering would require an efficient method for editing the genomes of  
114 primary isolates, we started by developing a new genetic system for *S. epidermidis*. By integrating  
115 elements of electroporation-based protocols for Gram-positive bacteria and yeast<sup>31–34</sup>, we developed a  
116 protocol with three key elements: to prepare electrocompetent cells, we cultivate *S. epidermidis* in  
117 hyperosmolar sorbitol, washing thoroughly in high volume 10% glycerol; to prepare the DNA, we pass the  
118 plasmid through a the methylase-deficient ( $\Delta$ *dcm*) *E. coli* strain DC10B<sup>24</sup>; and directly before (Method 1)  
119 or after (Method 2) electroporation, we introduce a heat shock (**Figure 1A**). Using this method, we were  
120 able to construct mutations in 13 of the 17 *S. epidermidis* strains we tested, include >10 primary human  
121 isolates from diverse phylogenetic groups (**Figure 1B**). Our approach does not restrict the efficiency of  
122 cloning to phage type and does not require specialized knowledge of strain-specific restriction systems.

123

## 124 **Engineering antigen expression into *S. epidermidis***

125 We used this system to engineer *S. epidermidis* LM087 (hereafter, *S. epidermidis*) to express non-  
126 native antigens, with the goal of redirecting T cell responses against an antigen of choice. Notably, the  
127 process by which *S. epidermidis* antigens are presented to CD8+ T cells is not well understood: the identity  
128 of the antigen-presenting cell is unclear, the mechanism by which antigen is presented on class I MHC  
129 (active transport from the cytosol vs. cross-presentation) is unknown, and the process that determines  
130 which antigens are selected from among thousands of proteins in the bacterial cell has not been studied.  
131 Additionally, it was unclear whether a non-native protein could compete against native *S. epidermidis*  
132 antigens for CD8+ T cell recognition, and if the foreign antigen would require presentation by the  
133 nonclassical MHC Ib molecule H2-M3, which presents immunodominant native *S. epidermidis* antigens to  
134 CD8+ T cells<sup>15</sup>.

135 Our strategy took these elements of uncertainty into account (**Figure 1C**). We started with  
136 ovalbumin (OVA) as a model tumor antigen since it harbors well-characterized antigenic peptides that are  
137 recognized by OVA-specific CD8+ or CD4+ T cells (OT-1 or OT-2, respectively). In light of the inherent  
138 challenges in expressing a non-native antigen in an undomesticated human isolate at high enough levels  
139 to be efficiently presented on MHC upon engulfment, we used a *Staphylococcus* replicative plasmid with  
140 a constitutive promoter (pLI50-P<sub>pen</sub>)<sup>35</sup> and added the ribosome binding site from the *S. aureus* delta-  
141 hemolysin (*hld*) gene, which promotes strong, constitutive translation in *S. aureus* and *S. epidermidis*<sup>36,37</sup>.  
142 We designed four forms of the OVA antigen: the full-length protein (OVA), an MHC I-restricted antigen  
143 from OVA (amino acids 257-264, here termed 'OT1'), an MHC II-restricted antigen from OVA (amino acids  
144 329-337, here termed 'OT2'), or a concatemer of three computationally predicted H2-M3-binding peptides  
145 from OVA ('OVA3pep')<sup>38</sup>. All forms of the OVA antigen were codon-optimized for *Staphylococcus*.

146 Next, we generated three sets of strains in which we varied the nature of the antigen and its  
147 subcellular localization within *S. epidermidis*: (i) One strain for cytoplasmic expression consisting solely of  
148 full-length OVA (cOVA). (ii) Four strains for cell-wall-displayed antigen in which OVA, OT1, OT2, or  
149 OVA3pep is spliced between the *N*-terminal sortase signal peptide and *C*-terminal cell wall-spanning  
150 regions of *S. aureus* protein A, yielding *S. epi-wOVA*, *S. epi-wOT1*, *S. epi-wOT2*, and *S. epi-wOVA3pep*.  
151 A similar approach has been used for surface display of recombinant proteins in *Staphylococcus xylosus*<sup>39</sup>.  
152 (iii) Eight strains for antigen secretion. In six of these strains, OT1, OT2, or OVA3pep are spliced into the  
153 secreted proteins FepB (Tat pathway)<sup>40,41</sup> or SERP0318 (Sec pathway)<sup>42</sup> at the predicted signal sequence  
154 cleavage site; in the remaining two, full-length OVA is fused to the *N*-terminal Tat or Sec signal sequences  
155 from the same proteins. The OVA-FepB chimeras yielded strains *S. epi-sOT1*, *S. epi-sOT2*, *S. epi-*  
156 *sOVA3pep*, and *S. epi-sOVA*; the OVA-SERP0318 chimeras expressed poorly and were not used further.

157 We verified production of the full-length OVA constructs by Western blot (**Figure S1**). Notably,  
158 although *S. epidermidis* has a well-described Sec secretion system and no discernible Tat secretion  
159 system, the Tat signal peptide enabled efficient production and secretion of OVA.

160

## 161 **Engineered strains of *S. epidermidis* stimulate antigen-specific T cells in vitro**

162 To test whether the engineered strains of *S. epidermidis* are capable of generating an antigen-  
163 specific CD8+ or CD4+ T cell response, we used an in vitro mixed lymphocyte assay in which the bacterial  
164 strain is mixed with murine dendritic cells and transgenic OT-1 or OT-2 T cells that are specific for an OVA  
165 peptide-MHC complex (**Figure 2A, S2**). We measured T cell activation after four hours of co-culture by  
166 monitoring the level of Nur77, an early and specific marker of T cell receptor signaling<sup>43</sup>.

167 From these data, we draw two conclusions: First, several of our engineered strains stimulate  
168 antigen-specific CD8+ and CD4+ T cells robustly, demonstrating that a non-native protein can be  
169 expressed at a high enough level in this undomesticated commensal to be presented by MHC I and II  
170 (**Figure 2B**).

171 Second, the subcellular localization of the antigen can dictate a preference toward CD8+ versus  
172 CD4+ T cell stimulation. The strain expressing cell wall-attached OVA (*S. epi-wOVA*) induces OVA-specific  
173 CD8+ T cells (OT-1) more efficiently than secreted OVA (*S. epi-sOVA*); in contrast, *S. epi-sOVA*  
174 preferentially stimulates OVA-specific CD4+ T cells (OT-2) (**Figure 2B**). The strain expressing cytoplasmic  
175 OVA (*S. epi-cOVA*) activates CD8+ and CD4+ T cells weakly even though cOVA is expressed at  
176 comparable levels to sOVA (**Figure S1**). Notably, strains expressing an OVA peptide rather than the full-  
177 length protein (*S. epi-wOT1*, *S. epi-wOT2*, *S. epi-sOT1*, and *S. epi-sOT2*) stimulate CD8+ or CD4+ T cells  
178 at high levels regardless of antigen localization.

179

## 180 ***S. epidermidis*-OVA slows the progression of subcutaneous melanoma**

181 Next, we tested the ability of the engineered *S. epidermidis* strains to limit the growth of tumor cells  
182 in a syngeneic model of murine melanoma (**Figure 3A**). Given our uncertainty about which T cell subtypes  
183 would be involved in antitumor immunity, wild-type specific pathogen free (SPF) C57BL/6 mice were  
184 colonized with a combination of *S. epi-wOT1* and *S. epi-sOVA* (hereafter, '*S. epi-OVA*'). Bacterial strains  
185 were transferred by gentle topical application to the top of the head using a cotton swab; as established  
186 previously, this procedure does not breach the skin barrier but leads to robust skin colonization by live  
187 bacteria<sup>23</sup>. Mice were colonized starting seven days before we subcutaneously injected cells from a  
188 C57BL/6-derived melanoma line that expresses ovalbumin, B16-F0-OVA, into the right flank. We did not  
189 administer additional immune adjuvant therapy (e.g., checkpoint blockade, cytokines, or adoptively  
190 transferred T cells). An *S. epidermidis* strain producing a control protein, mCherry, from the same plasmid  
191 backbone was applied topically as a control (*S. epi-control*).

192 *S. epi-OVA* elicited a marked reduction in tumor growth (**Figure 3B**). Nonspecific CD8+ T cell  
193 induction by the control strain had no apparent effect; tumors grew just as quickly in *S. epi-control*-treated  
194 mice compared to naïve SPF mice (**Figure 3B**). Additionally, although the overall levels of CD4+ and CD8+



195 T cells are comparable in the tumor-draining lymph nodes, the percentage of IFN $\gamma$ -expressing CD4+ and  
196 CD8+ T cells increase following colonization with *S. epi-OVA* but not *S. epi-control* (**Figure 3C**). The tumor-  
197 draining lymph nodes also contain an increased percentage of OVA-specific CD8+ T cells as measured  
198 by H2-Kb/SIINFEKL tetramer staining (**Figure 3C**). These results suggest that *S. epi-OVA* elicits an  
199 antitumor immune response under conditions of physiologic colonization. Moreover, OVA-expressing  
200 colonists induce activated, antigen-specific CD4+ and CD8+ T cells that migrate to the tumor.

201 Three additional results begin to clarify cellular requirements for the host and microbial colonist.  
202 First, heat-killed *S. epi-OVA* failed to stimulate an antitumor response (**Figure 3D**), suggesting that the  
203 engineered bacterial colonist is not simply a source of antigen and adjuvant; bacterial viability and  
204 (potentially) prolonged antigen exposure are required for the immune stimulatory response, even though  
205 no infection is mounted.

206 Second, antibody-mediated depletion of CD8+ T cells or all TCR $\beta$ + cells eliminates the antitumor  
207 effect, consistent with a role for CD8+ and CD4+ T cells in the *S. epi-OVA*-induced response (**Figures 3D**  
208 and **S3**).

209 Finally, the subcellular localization of the antigen in *S. epidermidis* can direct a CD8+ versus CD4+  
210 T cell response *in vivo* (**Figure 3E**). To determine the localization and antigen requirements for the  
211 antitumor effect, we colonized mice with *S. epidermidis* strains harboring different versions of OVA before  
212 injecting B16-OVA tumor cells subcutaneously into the right flank. Since *S. epi-wOT1* only contains the  
213 CD8+ T cell antigen, we colonized mice with *S. epi-wOVA*—which contains full-length OVA—to determine  
214 whether a wall-displayed construct with CD8+ and CD4+ antigens could elicit a response. However, *S.*  
215 *epi-wOVA* showed no antitumor effect compared to control. In contrast, colonization with a combination of  
216 *S. epi-wOT1* and *S. epi-sOT2* decreased tumor size and increased IFN $\gamma$ -expressing CD8+ T cells (**Figure**  
217 **3F**), suggesting that the minimal requirements for antitumor efficacy are a wall-attached CD8+ antigen and  
218 a secreted CD4+ antigen. When we mismatch the localization and antigenic peptide identity by colonizing  
219 with *S. epi-wOT2* and *S. epi-sOT1*, the antitumor effect is lost (**Figure 3E**) and IFN $\gamma$ -expressing CD4+ and  
220 CD8+ T cells are not increased in the tumor-draining lymph node (**Figure 3F**). In contrast to the findings  
221 from our *in vitro* assay (**Figure 2B**), these *in vivo* data are consistent with a model in which antigen  
222 localization in the bacterial cell is critical: a wall-attached CD8+ epitope and a secreted CD4+ epitope are  
223 necessary for optimal antitumor activity. These results also suggest that antigen-specific CD4+ and CD8+  
224 T cells are both required for the *S. epidermidis*-induced antitumor response.

225

### 226 **The antitumor effect of *S. epidermidis* extends to metastases outside the skin compartment**

227 In the previous experiments, tumor cells were injected into the subcutaneous tissue of the flank.  
228 Although mice were colonized by topical application to the head, murine grooming behavior could distribute

229 *S. epidermidis* broadly across the skin, raising the question of whether the bacterial colonist and the tumor  
230 need to be in close proximity for the induction of an antitumor immune response.

231 To address this question, we performed a similar experiment in the setting of metastatic melanoma  
232 using a cell line derived from B16-F10, a well-characterized (and more aggressive) variant of B16  
233 melanoma. B16-F10-OVA cells constitutively expressing luciferase were injected intravenously rather than  
234 subcutaneously, resulting in metastases to the lungs (**Figure 4A**). Topical association with *S. epi*-OVA  
235 seven days prior to intravenous tumor cell injection slowed tumor progression substantially (**Figure 4C-E,**  
236 **S4**), demonstrating that the antitumor effect of *S. epi*-OVA is not restricted to skin and subcutaneous  
237 tissues. These data suggest that the antitumor effect of antigen-expressing *S. epidermidis* does not require  
238 an infection or proximity to the tumor.

239

### 240 ***S. epidermidis* producing a native neoantigen slows melanoma progression**

241 Model antigens are useful for studying the specificity of an adaptive immune response, but their  
242 efficient processing in antigen-presenting cells and high expression in syngeneic tumor cell lines raises  
243 the question of whether this approach would work in the more realistic setting of a neoantigen naturally  
244 present in a tumor. To address this question, we engineered *S. epidermidis* to express two neoantigen-  
245 containing peptides naturally present in B16-F10 melanoma cells and previously reported to drive an  
246 antitumor response when formulated as an mRNA vaccine<sup>44</sup> (**Figure 4B**). The neoantigen peptide from  
247 Obsl1(T1764M) stimulates CD8+ T cells preferentially, so we spliced a 27-aa peptide centered around the  
248 mutated residue into the wall-attachment scaffold, yielding strain *S. epi*-wB16Ag. The other neoantigen  
249 peptide, Ints11(D314N), primarily stimulates CD4+ T cells, so we spliced a 27-aa peptide harboring the  
250 mutation into a scaffold for Tat-mediated secretion, generating strain *S. epi*-sB16Ag.

251 We colonized mice with a mixture of *S. epi*-wB16Ag and *S. epi*-sB16Ag (termed '*S. epi*-neoAg')  
252 and then injected the mice intravenously with B16-F10-OVA-luc cells seven days later. In contrast to *S.*  
253 *e**pi*-control, which failed to reduce tumor size, *S. epi*-neoAg restricted tumor growth at a comparable level  
254 to *S. epi*-OVA (**Figure 4C-E, S4**). Mice colonized by *S. epi*-neoAg do not exhibit any symptoms of  
255 autoimmunity, consistent with a model in which *S. epidermidis*-induced T cells are selective for tumor cells  
256 over healthy tissue. These data suggest that commensal-induced T cells can be redirected against a  
257 potentially broad range of host antigens.

258

## 259 **DISCUSSION**

260 Our findings are consistent with a model in which an engineered commensal induces antigen-  
261 specific T cells (**Figure 4F**). Once they are primed by antigen, possibly in the skin-draining lymph nodes,  
262 these T cells can migrate to the tumor and kill tumor cells. Thus, we have co-opted the barrier response to



263 a commensal and redirected it against a tumor, protecting the host against local and metastatic tumor  
264 progression.

265 Our approach—using a commensal microbe as the adjuvant and colonization as the mode of  
266 delivery in a tumor vaccine—differs from previous approaches in important ways. It does not result in an  
267 infection or require intratumoral delivery, so it is safer, simpler, and more specific than approaches that  
268 require inflammation or tissue infiltration for antitumor activity. Additionally, heat-killed *S. epi-OVA* fails to  
269 elicit a response, so we are not simply administering a purified antigen and adjuvant. The need for live  
270 bacteria suggests that *S. epidermidis* engages the immune system’s powerful (if incompletely understood)  
271 ‘barrier program’, in which the host pre-emptively develops an adaptive immune response against microbial  
272 colonists. A strain that colonizes stably may lead to prolonged antigen exposure—the equivalent of a  
273 ‘prime’ and a constant ‘boost’—and, as a result, a robust memory immune cell response.

274 The immune response we elicit is complex and controllable. Engineered strains of *S.*  
275 *epidermidis* induce a combination of antigen-specific CD8+ and CD4+ T cells; both are required for  
276 antitumor activity, consistent with recent work in the context of a neoantigen vaccine<sup>45</sup>. Moreover, by  
277 expressing antigens in different compartments of the bacterial cell, we can independently control the  
278 specificity of CD8+ and CD4+ T cell responses, a powerful capability that could be used to drive  
279 multifaceted responses against multiple antigens in distinct tissues.

280 Two improvements in design could make our approach more efficacious. First, although we  
281 observed efficacy without the need for adjuvant checkpoint blockade or cytokine therapy, combining  
282 antigen-expressing *S. epidermidis* strains with, e.g., antibodies targeting PD-1 or CTLA-4 could yield even  
283 more robust responses. Second, most of our experiments targeted one or two antigens in the tumor,  
284 leaving open the possibility of T cell escape by downregulating or mutating the antigen. Neoantigen  
285 vaccines typically use a small library of antigens; adapting a similar approach here would be  
286 straightforward and could improve efficacy and limit the possibility of antigen escape.

287 Finally, two results show the potential generality of our approach. First, engineered *S.*  
288 *epidermidis* protects against the growth of metastatic melanoma, so there is no need for physical proximity  
289 between the bacterium and the tumor. As a result, engineered commensal vaccines may be well suited to  
290 solid tumors and have a chance of working in a variety of tumors to which T cells have access. Second,  
291 the efficacy of neoantigen-expressing strains of *S. epidermidis* shows that our approach is not limited to  
292 model antigens; any immunogenic tumor antigen could work.

293 More broadly, it might be possible to engineer antigen expression into other commensal bacterial  
294 strains to elicit a wide range of antigen-specific immune cell responses. The barrier response to  
295 commensal bacteria consists of multiple adaptive immune cell types that are induced simultaneously and  
296 work together. Understanding how to redirect each one may open the door to immunotherapies for  
297 other diseases.

## 298 REFERENCES

299

- 300 1. Ribas, A. & Wolchok, J. D. Cancer immunotherapy using checkpoint blockade. *Science* **359**, 1350–  
301 1355 (2018).
- 302 2. June, C. H., Warshauer, J. T. & Bluestone, J. A. Is autoimmunity the Achilles' heel of cancer  
303 immunotherapy? *Nat. Med.* **23**, 540–547 (2017).
- 304 3. Michot, J. M. *et al.* Immune-related adverse events with immune checkpoint blockade: a  
305 comprehensive review. *Eur. J. Cancer* **54**, 139–148 (2016).
- 306 4. June, C. H., O'Connor, R. S., Kawalekar, O. U., Ghassemi, S. & Milone, M. C. CAR T cell  
307 immunotherapy for human cancer. *Science* **359**, 1361–1365 (2018).
- 308 5. Sadelain, M., Rivièrè, I. & Riddell, S. Therapeutic T cell engineering. *Nature* **545**, 423–431 (2017).
- 309 6. Prasad, V. Immunotherapy: Tisagenlecleucel - the first approved CAR-T-cell therapy: implications  
310 for payers and policy makers. *Nat. Rev. Clin. Oncol.* **15**, 11–12 (2018).
- 311 7. Long, A. H. *et al.* 4-1BB costimulation ameliorates T cell exhaustion induced by tonic signaling of  
312 chimeric antigen receptors. *Nat. Med.* **21**, 581–590 (2015).
- 313 8. Newick, K., O'Brien, S., Moon, E. & Albelda, S. M. CAR T cell therapy for solid tumors. *Annu. Rev.*  
314 *Med.* **68**, 139–152 (2017).
- 315 9. Sahin, U. & Türeci, Ö. Personalized vaccines for cancer immunotherapy. *Science* **359**, 1355–1360  
316 (2018).
- 317 10. Carreno, B. M. *et al.* Cancer immunotherapy. A dendritic cell vaccine increases the breadth and  
318 diversity of melanoma neoantigen-specific T cells. *Science* **348**, 803–808 (2015).
- 319 11. Nestle, F. O. *et al.* Vaccination of melanoma patients with peptide- or tumor lysate-pulsed dendritic  
320 cells. *Nat. Med.* **4**, 328–332 (1998).
- 321 12. Perez, C. R. & De Palma, M. Engineering dendritic cell vaccines to improve cancer immunotherapy.  
322 *Nat. Commun.* **10**, 5408 (2019).
- 323 13. Yang, Y. *et al.* Focused specificity of intestinal TH17 cells towards commensal bacterial antigens.  
324 *Nature* **510**, 152–156 (2014).
- 325 14. Xu, M. *et al.* c-MAF-dependent regulatory T cells mediate immunological tolerance to a gut  
326 pathobiont. *Nature* **554**, 373–377 (2018).
- 327 15. Linehan, J. L. *et al.* Non-classical Immunity Controls Microbiota Impact on Skin Immunity and Tissue  
328 Repair. *Cell* **172**, 784–796.e18 (2018).
- 329 16. Hegazy, A. N. *et al.* Circulating and Tissue-Resident CD4+ T Cells With Reactivity to Intestinal  
330 Microbiota Are Abundant in Healthy Individuals and Function Is Altered During Inflammation.  
331 *Gastroenterology* **153**, 1320–1337.e16 (2017).
- 332 17. Nishikawa, H. *et al.* In vivo antigen delivery by a Salmonella typhimurium type III secretion system  
333 for therapeutic cancer vaccines. *J. Clin. Invest.* **116**, 1946–1954 (2006).
- 334 18. Stark, F. C., Sad, S. & Krishnan, L. Intracellular bacterial vectors that induce CD8(+) T cells with  
335 similar cytolytic abilities but disparate memory phenotypes provide contrasting tumor protection.  
336 *Cancer Res.* **69**, 4327–4334 (2009).
- 337 19. Wood, L. M. & Paterson, Y. Attenuated *Listeria monocytogenes*: a powerful and versatile vector for  
338 the future of tumor immunotherapy. *Front. Cell Infect. Microbiol.* **4**, 51 (2014).
- 339 20. Chowdhury, S. *et al.* Programmable bacteria induce durable tumor regression and systemic  
340 antitumor immunity. *Nat. Med.* **25**, 1057–1063 (2019).
- 341 21. Leventhal, D. S. *et al.* Immunotherapy with engineered bacteria by targeting the STING pathway for  
342 anti-tumor immunity. *Nat. Commun.* **11**, 2739 (2020).
- 343 22. Naik, S. *et al.* Commensal-dendritic-cell interaction specifies a unique protective skin immune  
344 signature. *Nature* **520**, 104–108 (2015).
- 345 23. Naik, S. *et al.* Compartmentalized control of skin immunity by resident commensals. *Science* **337**,  
346 1115–1119 (2012).
- 347 24. Monk, I. R., Shah, I. M., Xu, M., Tan, M.-W. & Foster, T. J. Transforming the untransformable:  
348 application of direct transformation to manipulate genetically *Staphylococcus aureus* and  
349 *Staphylococcus epidermidis*. *MBio* **3**, (2012).

- 350 25. Winstel, V., Kühner, P., Krismer, B., Peschel, A. & Rohde, H. Transfer of plasmid DNA to clinical  
351 coagulase-negative staphylococcal pathogens by using a unique bacteriophage. *Appl. Environ.*  
352 *Microbiol.* **81**, 2481–2488 (2015).
- 353 26. Lee, J. Y. H. *et al.* Functional analysis of the first complete genome sequence of a multidrug  
354 resistant sequence type 2 *Staphylococcus epidermidis*. *Microb. Genom.* **2**, e000077 (2016).
- 355 27. Monk, I. R., Tree, J. J., Howden, B. P., Stinear, T. P. & Foster, T. J. Complete Bypass of Restriction  
356 Systems for Major *Staphylococcus aureus* Lineages. *MBio* **6**, e00308-15 (2015).
- 357 28. Moran, J. L., Dingari, N. N., Garcia, P. A. & Buie, C. R. Numerical study of the effect of soft layer  
358 properties on bacterial electroporation. *Bioelectrochemistry* **123**, 261–272 (2018).
- 359 29. Winstel, V. *et al.* Wall teichoic acid structure governs horizontal gene transfer between major  
360 bacterial pathogens. *Nat. Commun.* **4**, 2345 (2013).
- 361 30. Winstel, V., Kühner, P., Rohde, H. & Peschel, A. Genetic engineering of untransformable coagulase-  
362 negative staphylococcal pathogens. *Nat. Protoc.* **11**, 949–959 (2016).
- 363 31. Augustin, J. & Götz, F. Transformation of *Staphylococcus epidermidis* and other staphylococcal  
364 species with plasmid DNA by electroporation. *FEMS Microbiol. Lett.* **54**, 203–207 (1990).
- 365 32. Manivasakam, P. & Schiestl, R. H. High efficiency transformation of *Saccharomyces cerevisiae* by  
366 electroporation. *Nucleic Acids Res.* **21**, 4414–4415 (1993).
- 367 33. van der Rest, M. E., Lange, C. & Molenaar, D. A heat shock following electroporation induces highly  
368 efficient transformation of *Corynebacterium glutamicum* with xenogeneic plasmid DNA. *Appl.*  
369 *Microbiol. Biotechnol.* **52**, 541–545 (1999).
- 370 34. Löfblom, J., Kronqvist, N., Uhlén, M., Ståhl, S. & Wernérus, H. Optimization of electroporation-  
371 mediated transformation: *Staphylococcus carnosus* as model organism. *J. Appl. Microbiol.* **102**,  
372 736–747 (2007).
- 373 35. Swoboda, J. G. *et al.* Discovery of a small molecule that blocks wall teichoic acid biosynthesis in  
374 *Staphylococcus aureus*. *ACS Chem. Biol.* **4**, 875–883 (2009).
- 375 36. Malone, C. L. *et al.* Fluorescent reporters for *Staphylococcus aureus*. *J. Microbiol. Methods* **77**, 251–  
376 260 (2009).
- 377 37. Franke, G. C. *et al.* Expression and functional characterization of gfpmut3.1 and its unstable variants  
378 in *Staphylococcus epidermidis*. *J. Microbiol. Methods* **71**, 123–132 (2007).
- 379 38. Chun, T. *et al.* Induction of M3-restricted cytotoxic T lymphocyte responses by N-formylated  
380 peptides derived from *Mycobacterium tuberculosis*. *J. Exp. Med.* **193**, 1213–1220 (2001).
- 381 39. Hansson, M. *et al.* Expression of recombinant proteins on the surface of the coagulase-negative  
382 bacterium *Staphylococcus xylosus*. *J. Bacteriol.* **174**, 4239–4245 (1992).
- 383 40. Biswas, L. *et al.* Role of the twin-arginine translocation pathway in *Staphylococcus*. *J. Bacteriol.* **191**,  
384 5921–5929 (2009).
- 385 41. Turlin, E., Débarbouillé, M., Augustyniak, K., Gilles, A.-M. & Wandersman, C. *Staphylococcus*  
386 *aureus* FepA and FepB proteins drive heme iron utilization in *Escherichia coli*. *PLoS One* **8**, e56529  
387 (2013).
- 388 42. Powers, M. E. *et al.* Type I signal peptidase and protein secretion in *Staphylococcus epidermidis*. *J.*  
389 *Bacteriol.* **193**, 340–348 (2011).
- 390 43. Ashouri, J. F. & Weiss, A. Endogenous nur77 is a specific indicator of antigen receptor signaling in  
391 human T and B cells. *J. Immunol.* **198**, 657–668 (2017).
- 392 44. Kreiter, S. *et al.* Mutant MHC class II epitopes drive therapeutic immune responses to cancer.  
393 *Nature* **520**, 692–696 (2015).
- 394 45. Alspach, E. *et al.* MHC-II neoantigens shape tumour immunity and response to immunotherapy.  
395 *Nature* **574**, 696–701 (2019).
- 396

397 **ACKNOWLEDGMENTS**

398 We are deeply indebted to members of the Fischbach Group for helpful suggestions and comments  
399 on the manuscript. We thank Yasmine Belkaid and members of her lab for useful discussions. We thank  
400 the Stanford animal facility staff for help with animal husbandry. Cell sorting and flow cytometry analyses  
401 were performed on instruments in the Stanford Shared FACS Facility with help from M. Weglarz. *S.*  
402 *epidermidis* strain NIHLM087 was a gift from Julie Segre and Yasmine Belkaid, NIH. pMS182 (pLI50-Ppen-  
403 GFP-mut2) was a gift from Suzanne Walker, Harvard University. B16-F0-OVA was a gift from Nathan  
404 Reticker-Flynn from the lab of Edgar Engleman, Stanford University. This work was supported by the  
405 Stanford Microbiome Therapies Initiative, an HHMI Hanna H. Gray Fellowship (Y.E.C.); an HHMI-Simons  
406 Faculty Scholar Award (M.A.F.); a Fellowship for Science and Engineering from the David and Lucile  
407 Packard Foundation (M.A.F.); an Investigators in the Pathogenesis of Infectious Disease award from the  
408 Burroughs Wellcome Foundation (M.A.F.); NIH grant DK110174 (M.A.F.); the Chan Zuckerberg Biohub  
409 (M.A.F.); the Human Frontier Science Program LT000493/2018-L (K.N.) and the Fellowship of Astellas  
410 Foundation for Research on Metabolic Disorders (K.N.).

411

412 **AUTHOR CONTRIBUTIONS**

413 Y.E.C., K.N., and M.A.F. conceived and designed the experiments. Y.E.C., K.A., and A.D.  
414 performed the experiments. Y.E.C. and M.A.F. analyzed data and wrote the manuscript. All authors  
415 discussed the results and commented on the manuscript.

416

417 **COMPETING INTERESTS**

418 M.A.F. is a co-founder and director of Federation Bio, a company developing microbiome-based  
419 therapeutics. Y.E.C. and K.N. are consultants for Federation Bio.

420

421 **SUPPLEMENTARY MATERIALS**

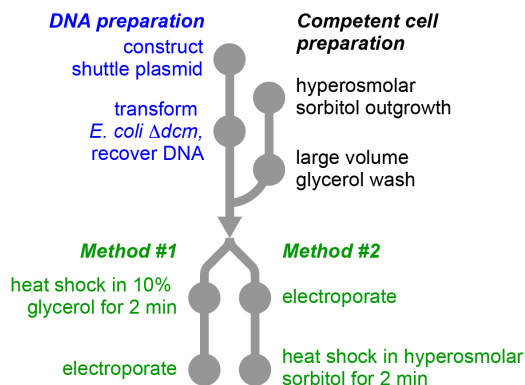
422 Materials and Methods

423 Figures S1-S3

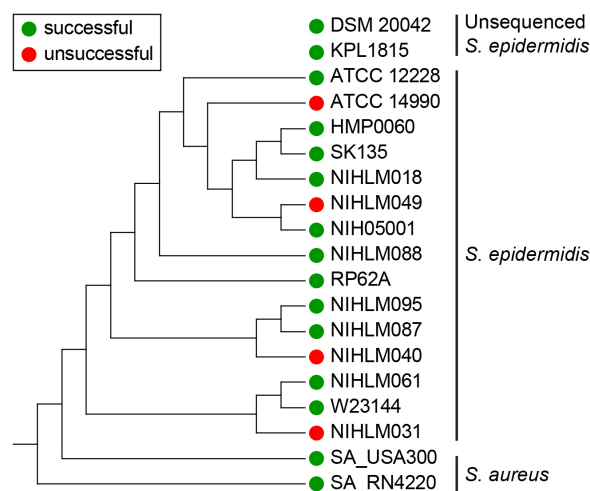
424 Table S1

Figure 1

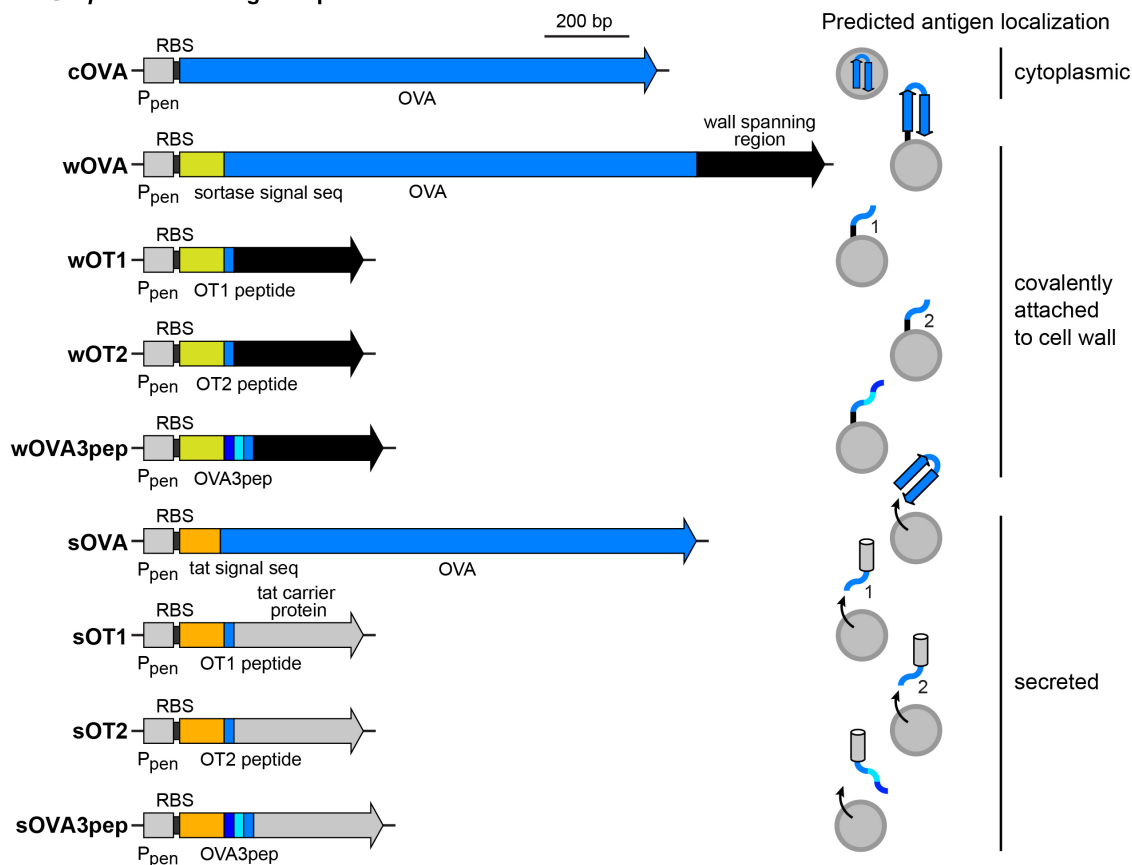
**A Method for engineering *S. epidermidis***



**B Genetic manipulation by strain**



**C *S. epidermidis* antigen expression constructs**



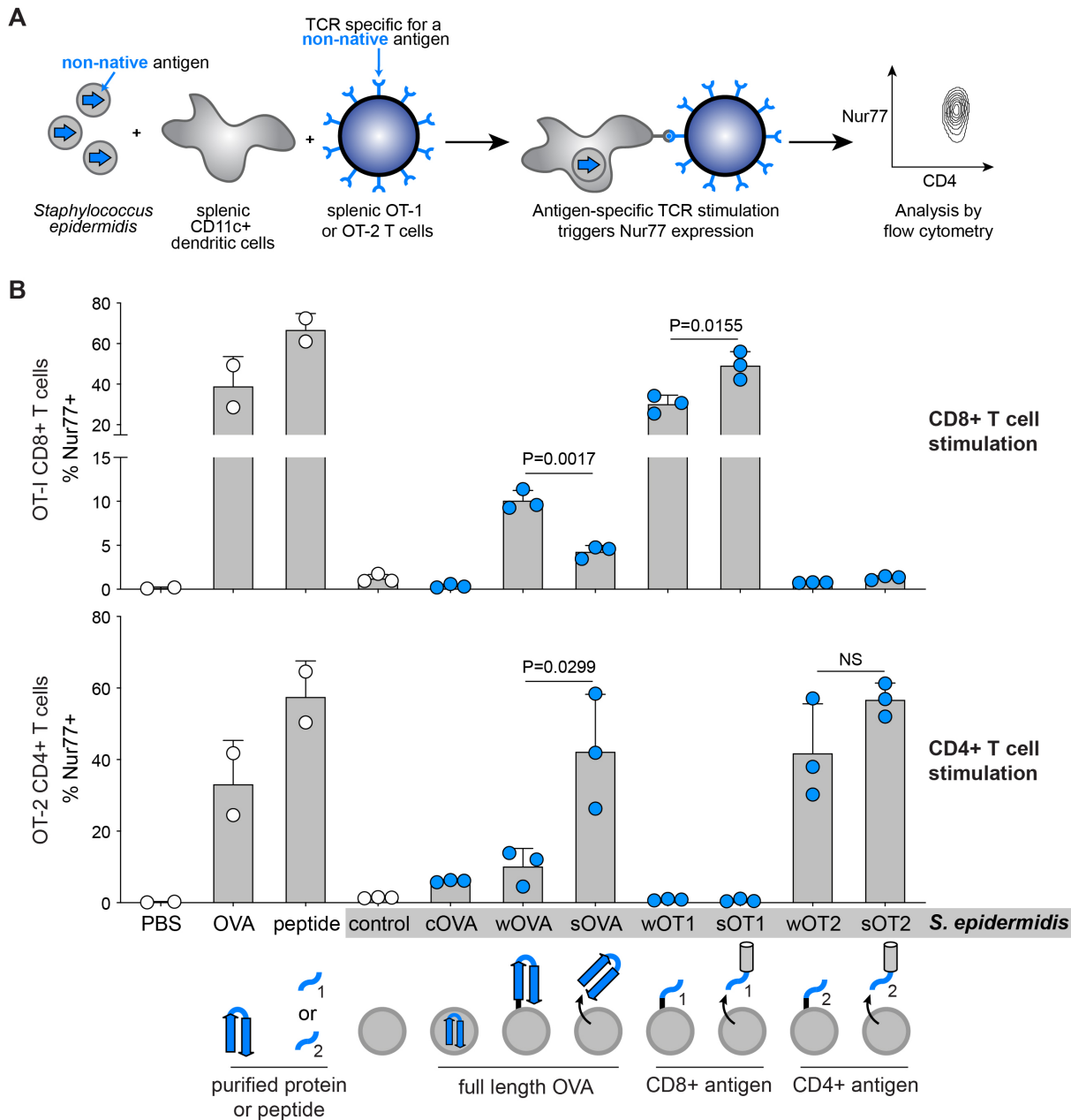
425  
 426

427 **Fig. 1. Engineering *S. epidermidis* to express non-native antigens.** (A) Schematic of the new genetic  
 428 system for *S. epidermidis*. To bypass stringent restriction systems, the target plasmid is passed through  
 429 *E. coli*  $\Delta dcm$ . To optimize cell competency, *S. epidermidis* is grown in media containing hyperosmolar  
 430 sorbitol, harvested during late-log phase, and thoroughly washed with a large volume of 10% glycerol to

431 eliminate salts. *Staphylococcus* is subjected to heat shock before (Method #1) or after (Method #2)  
432 electroporation with the plasmid. (B) Phylogenetic tree of *S. epidermidis* and *S. aureus* strains. This  
433 method was successful in 13 of the 17 primary *S. epidermidis* isolates in which we tested it, including two  
434 strains that do not have genome sequences available in NCBI. Green = genetically manipulatable. Red =  
435 not genetically manipulatable with our method. (C) We constructed strains in which full-length ovalbumin  
436 or an ovalbumin-derived peptide is expressed in the cytoplasm, fused to the cell wall, or secreted. The  
437 predicted subcellular localization of each antigen is shown at right. Expression is driven by the constitutive  
438 *S. aureus* promoter Ppen (gray box) and the ribosome binding site (RBS) from *S. aureus hld*. Ovalbumin  
439 (blue box) is expressed either as a full-length protein (OVA), the MHC I-restricted antigenic peptide (OT1),  
440 the MHC II-restricted antigenic peptide (OT2), or a concatemer of computationally predicted H2-M3-  
441 restricted antigenic peptides (OVA3pep). For localization to the cell wall, the antigen was inserted between  
442 the signal sequence from *S. aureus* protein A (yellow box) and a wall-spanning domain that is covalently  
443 anchored to the cell wall by sortase (black arrow). For secretion, full-length OVA without its N-terminal  
444 methionine is fused to the Tat signal sequence of *S. aureus fepB* (orange box) or an antigen-containing  
445 peptide is inserted into *fepB* immediately after the N-terminal signal sequence.



Figure 2



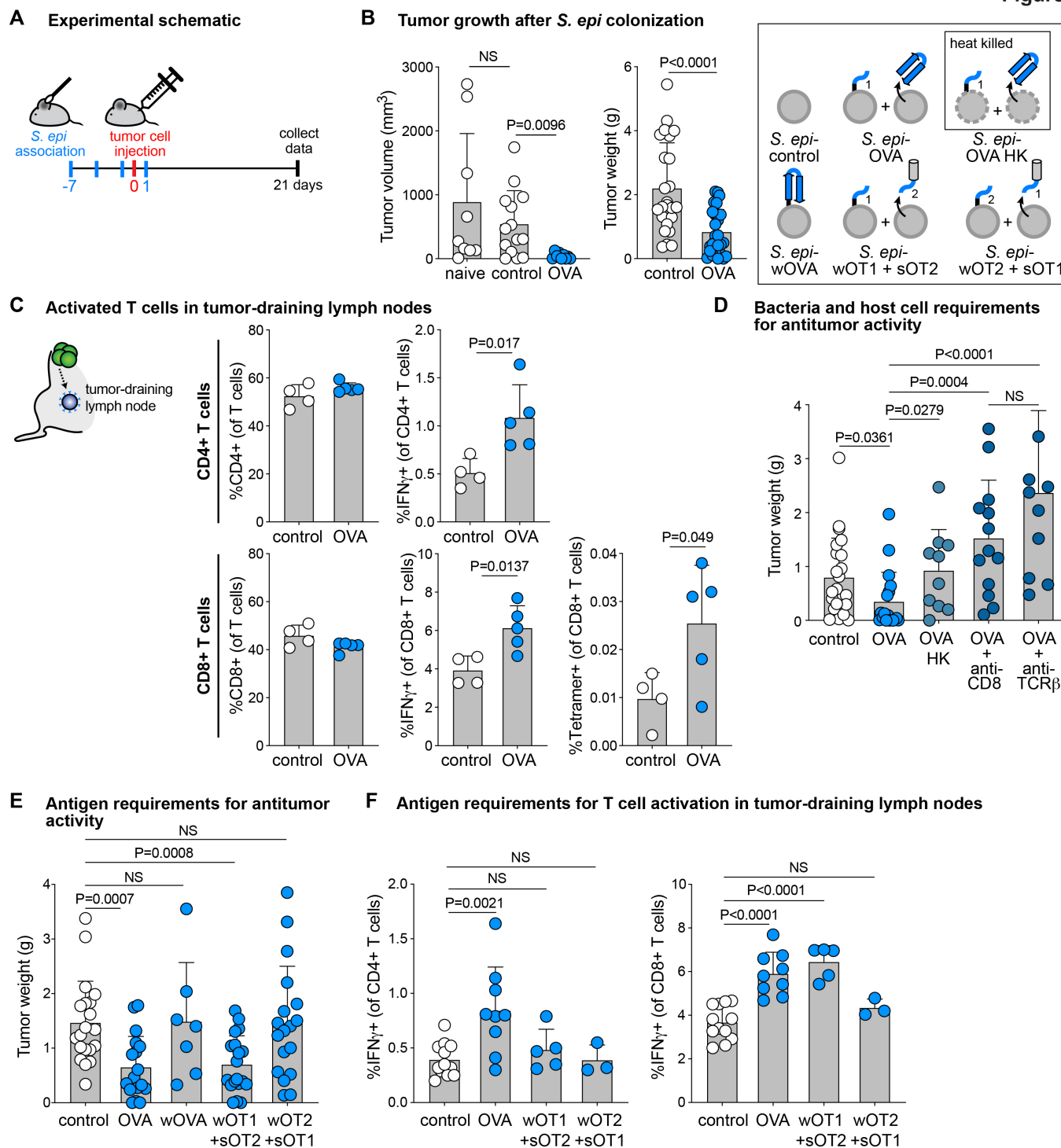
446

447

448 **Fig. 2. Engineered strains of *S. epidermidis* stimulate antigen-specific T cells in vitro.** (A) Schematic  
 449 of the in vitro assay of T cell activation. Each *S. epidermidis* strain is heat-shocked to prevent bacterial  
 450 overgrowth of mammalian cells and co-cultured with splenic CD45.1+ CD11c+ dendritic cells for two hours  
 451 to allow for antigen processing. Transgenic T cells specific for an OVA-derived CD8+ (OT-1) or CD4+ (OT-  
 452 2) T cell epitope are then added and co-cultured for four hours to enable antigen presentation from dendritic  
 453 cells to T cells and TCR signaling, which upregulates Nur77 expression. Cells are then placed on ice,  
 454 fixed, stained for surface markers and intracellular markers, and then analyzed by flow cytometry. T cells  
 455 are gated on live CD45.1- CD90.2+ TCRβ+ CD8β+ or CD4+ and analyzed for expression of Nur77, an

456 early marker of TCR signaling. (B) Percentage of Nur77+ CD8+ T cells (top) or Nur77+ CD4+ T cells  
457 (bottom) in the presence of PBS, purified ovalbumin (OVA), purified OT1 (top) or OT2 (bottom) peptide, or  
458 engineered *S. epidermidis* strains (highlighted in gray bar). Representative flow plots are shown in **Figure**  
459 **S1**.

Figure 3



460

461

462

463

464

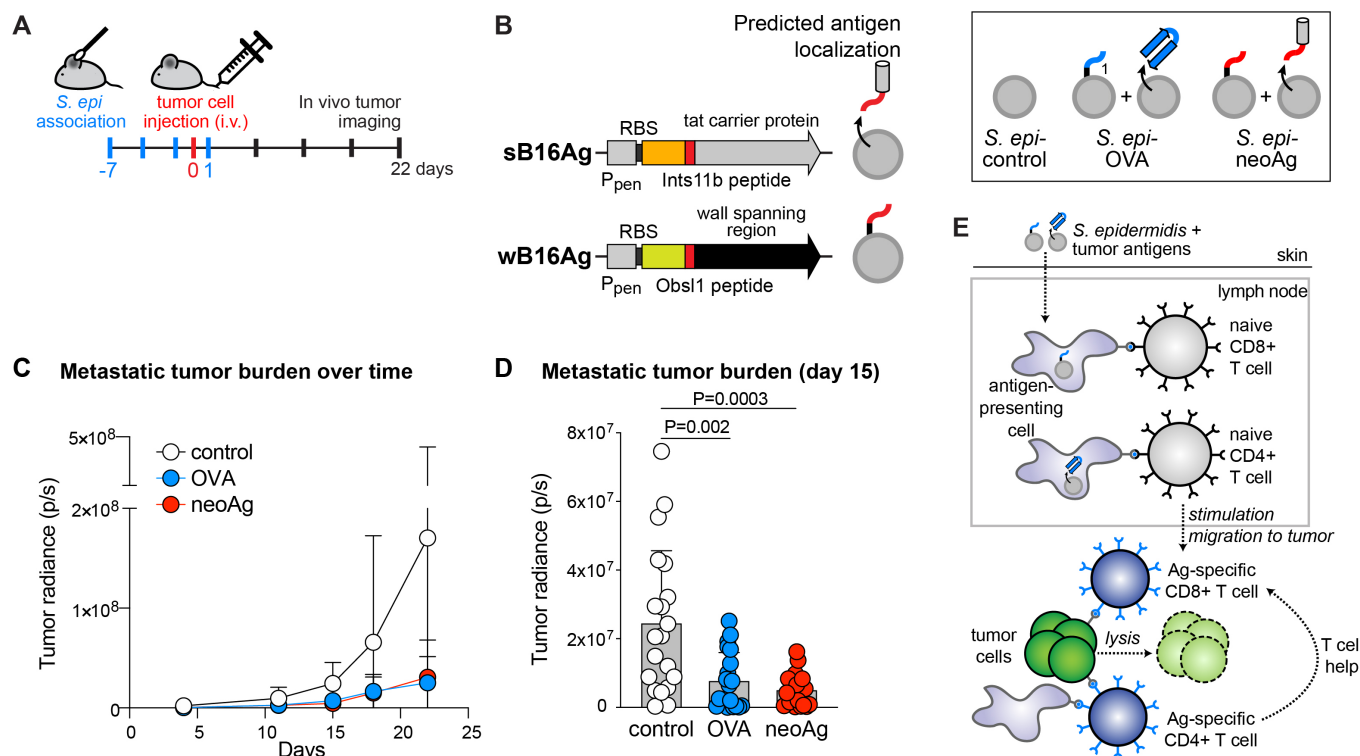
465

466

**Fig. 3. Engineered *S. epidermidis* strains slow tumor progression and stimulate antigen-specific T cells in vivo.** (A) Schematic of subcutaneous tumor experiments. Mice are colonized topically by gentle application of live *S. epidermidis* strains to the head with a cotton swab starting seven days prior to tumor injection. On day 0, B16-F0-OVA melanoma cells are freshly prepared from growing cultures and injected subcutaneously into the right flank. Mice are sacrificed on day 21, and tumors and tumor-draining inguinal

467 lymph nodes are collected for analysis. (B) Left panel: day 19 caliper measurements of subcutaneous B16-  
468 F0-OVA tumors in naïve SPF mice and mice colonized with *S. epi*-control or *S. epi*-OVA (a 1:1 mixture of  
469 *S. epi*-wOT1 and *S. epi*-sOVA). Right panel: day 21 masses of dissected subcutaneous tumors. (C) Flow  
470 cytometry analysis of tumor-draining inguinal lymph nodes. Frequencies of CD4<sup>+</sup> (top) and CD8<sup>+</sup> (bottom)  
471 cells within live CD90.2<sup>+</sup> TCRβ<sup>+</sup> T cells do not differ between control (white dots) and *S. epi*-OVA-  
472 associated (blue dots) mice, but frequencies of IFN-γ<sup>+</sup> cells increased within both CD4<sup>+</sup> T cells (top) and  
473 CD8<sup>+</sup> T cells (bottom). The frequency of MHC I-SIINFEKL tetramer<sup>+</sup> cells within CD8<sup>+</sup> T cells (bottom  
474 right) is increased in *S. epi*-OVA-colonized mice compared to control. (D) Masses of subcutaneous B16-  
475 F0-OVA tumors on day 21, dissected from *S. epi*-associated mice. *S. epi*-OVA-colonized mice were treated  
476 2x/week with intraperitoneal injections of 200 μg/mouse anti-CD8α (2.43) or anti-TCRβ (H57-597)  
477 neutralizing antibodies (dark blue dots). (E) Masses of subcutaneous B16-F0-OVA tumors on day 21 from  
478 *S. epi*-colonized mice. (F) Flow cytometry analysis of tumor-draining inguinal lymph nodes from mice  
479 shown in panel E. Frequencies of IFNγ<sup>+</sup> cells within live CD90.2<sup>+</sup> TCRβ<sup>+</sup> CD4<sup>+</sup> (left) or CD8<sup>+</sup> (right) T  
480 cells are shown. Data shown are representative of multiple independent experiments.

Figure 4



481

482

483

484

485

486

487

488

489

490

491

492

493

494

495

496

497

**Fig. 4. Efficacy of engineered *S. epidermidis* strains in metastatic melanoma.** (A) Schematic of metastatic melanoma experiments. Mice are colonized topically with live *S. epidermidis* strains starting 7 days prior to tumor injection. On day 0, B16-F10-OVA melanoma cells (which express luciferase constitutively) are freshly prepared from growing cultures and injected intravenously into the tail vein. The tumor burden in live mice is monitored 1-2x/week by intraperitoneal luciferin injection followed by bioluminescence imaging with an IVIS Lumina Imager. Mice are sacrificed on day 22. (B) Schematic of neoantigen expression constructs and their predicted subcellular localization within *S. epidermidis*. The wall-attachment and secretion scaffolds are identical to those for wOT1 and sOT1. The neoantigen coding sequence (red box) encodes 27-aa peptides centered around Obs1(T1764M) for the wall-attached construct (wB16Ag) or around Ints11(D314N) for the secreted construct (sB16Ag). (C) Quantification of tumor bioluminescence with dots showing the average measurement at each timepoint. (D) Bar graphs showing tumor bioluminescence on day 15 with each dot representing the measurement for each individual mouse. (E) Model of antitumor response induced by engineered commensals. Antigen-expressing strains of *S. epidermidis* colonize the skin and induce antigen-presenting cells to stimulate CD8+ or CD4+ T cells, respectively. Activated antigen-specific T cells then traffic to the tumor to restrict tumor growth.